

A new theory describing the hydrogen-assisted intergranular cracking of high-strength steels

JONG-KYO CHOI, SU-IL PYUN

Department of Materials Science and Engineering, Korea Advanced Institute of Science and Technology, PO Box 131 Chongyangni, Seoul, Korea

A thermodynamic analysis of hydrogen-assisted intergranular brittle fracture of high-strength steels has been made. In this analysis the functional relationship between cohesive energy and hydrogen coverage is derived in the case of solute equilibrium constraint during the decohering process. This relationship is evaluated and discussed in the presence of a triaxial stress field. The variation of threshold-stress intensity, K_{th} , with hydrogen fugacity is calculated by a criterion for hydrogen-assisted intergranular fracture, and is also considered as it relates to the effects of several material parameters, such as trap-binding energy at a grain boundary, yield strength and work-hardening exponent. In particular the fracture mode transition by hydrogen-assisted cracking is discussed as it relates to the effects of hydrogen on the K_{th} necessary for the occurrence of the respective fracture modes.

1. Introduction

It has been generally reported that steels are fractured in hydrogen gas or hydrogen-producing environments by the three fracture modes: micro-void coalescence, quasi-cleavage, and intergranular modes [1-5]. For higher-strength steels, the hydrogen-assisted cracking occurs in the intergranular mode, and the fractions of quasi-cleavage and micro-void coalescence modes on the hydrogen-assisted cracking fracture surface increase as the strength level is lowered [3, 4]. Since the intergranular hydrogen-assisted cracking requires the least fracture energy of the three fracture modes, it can cause dangerous failure to structures of high-strength steels in service. Therefore the investigation of the intergranular hydrogen-assisted cracking is of great importance from both engineering and scientific viewpoints.

In an effort to understand the hydrogen-assisted cracking process, the dependence of the threshold-stress intensity K_{th} (below which the cracking does not take place) on hydrogen fugacity or hydrogen concentration within the materials has been theoretically and experimentally investigated by several authors [6-12]. Most investigators represent different standpoints on this subject, and the theoretical relationship of cohesive strength against hydrogen concentration is not considered in their works. For a more reliable analysis of the hydrogen-assisted cracking process related to K_{th} against hydrogen fugacity, it is necessary to make a theoretical analysis of the relationship between cohesive strength and hydrogen coverage, and also to make analyses of the fracture mode transition as a function of stress intensity.

In evaluating the hydrogen concentration ahead of the crack tip, it is usually suggested that the presence of tensile hydrostatic stress enhances the concentration of hydrogen atoms in the fracture zone, which

results in the brittle fracture [6, 8, 10]. Recently, however, both hydrostatic stress and trap-binding energy have been taken into consideration as driving forces for hydrogen segregation [6, 7, 11-13].

The objectives of this present work are first, to obtain a functional relationship between cohesive energy and hydrogen coverage by a thermodynamic treatment, and second, to describe the intergranular hydrogen-assisted cracking process in terms of K_{th} and hydrogen fugacity with the help of the critical stress and critical hydrogen concentration concepts. The relationship of K_{th} against hydrogen fugacity is also discussed in relation to the effects of some material parameters, such as trap-binding energy at a grain boundary, yield strength and work-hardening exponent. Finally, the fracture mode transition in the hydrogen-assisted cracking process with varying stress intensity is conceptually established from the viewpoint of the known micro-mechanisms.

2. Dependence of surface energy and cohesive energy on hydrogen coverage

As a necessary criterion for the occurrence of a brittle fracture process, two conditions have been proposed [14],

$$\frac{\sigma_{max}}{\tau_{max}} > \frac{\sigma_{th}}{\tau_{th}} \quad (1a)$$

and

$$\sigma_{max} > \sigma_{th} \quad (1b)$$

where σ_{max} and τ_{max} are the maximum resolved normal and shear stresses, respectively, σ_{th} is the cohesive strength, and τ_{th} is the shear resistance of the material.

The criterion for brittle fracture is also applicable to intergranular hydrogen-assisted cracking, where σ_{th} is

given by

$$\sigma_{\text{th}} = \left[\frac{E(2\gamma_s - \gamma_b)}{2a_0} \right]^{1/2} \quad (2)$$

Where E is Young's modulus, a_0 is the lattice spacing, and γ_s and γ_b are the surface energies of the free surface and decohering grain boundary, respectively. When the shear resistance of the material τ_{th} is increased and/or the cohesive strength σ_{th} is reduced, Equations 1a and 1b are easily satisfied and a brittle fracture can occur even at a relatively low stress level. Intergranular decohesion is feasible only if σ_{max} is larger than the cohesive strength of grain boundary σ_{th} . Intergranular fracture thus requires the cohesive energy of a grain boundary, $2\gamma_s - \gamma_b$, to be reduced and/or σ_{max} at a grain boundary to be increased by the pile-up of immobile dislocations.

In this section, the functional relationship between cohesive energy of decohering grain boundary and hydrogen coverage is obtained for a crack equilibrated with hydrogen. We consider a mixture of iron and hydrogen containing 1 mole of total atoms, and also make a distinction between bulk phase, free surface and grain boundary which provide a hydrogen site i . The free energy of the mixture G_i can be written as follows,

$$G_i = (1 - f_i)\mu_0^{\text{Fe}} + f_i(\mu_0^{\text{H}} - H_i) - TS_i^{\text{conf}}$$

where f_i = atomic fraction of hydrogen; μ_0^{Fe} = molar free energy of pure iron; μ_0^{H} = molar free energy of pure hydrogen; H_i = molar enthalpy difference between pure hydrogen and hydrogen dissolved/adsorbed at the site i ; and S_i^{conf} = configurational entropy. It is assumed that energetic contributions other than that due to the configurational entropy are included in H_i . S_i^{conf} is given by

$$S_i^{\text{conf}} = -R \left\{ f_i \ln \left(\frac{f_i}{n_i^0} \right) - n_i^0 (1 - f_i) \ln (1 - f_i) + n_i^0 \left[1 - \frac{f_i(n_i^0 + 1)}{n_i^0} \right] \ln \left[1 - \frac{f_i(n_i^0 + 1)}{n_i^0} \right] \right\}$$

where R is the gas constant, and n_i^0 is the number of adsorption or trapping sites per atom of iron. If n_i is designated the number of adsorbed or trapped hydrogen atoms per atom of iron, f_i is equal to $n_i/(1 + n_i)$.

Now we define the fractional coverage of hydrogen at site i , θ_i , as the ratio of n_i/n_i^0 . From the Gibbs–Duhem equation, the chemical potentials of iron and hydrogen at site i are given by

$$\mu_i^{\text{Fe}} = \mu_0^{\text{Fe}} + n_i^0 RT \ln (1 - \theta_i) \quad (3a)$$

and

$$\mu_i^{\text{H}} = (\mu_0^{\text{H}} - H_i) + RT \ln \left(\frac{\theta_i}{1 - \theta_i} \right) \quad (3b)$$

respectively. At equilibrium, the chemical potentials of hydrogen are the same anywhere within the material. Hence

$$\frac{\theta_i}{1 - \theta_i} = \frac{\theta_L}{1 - \theta_L} \exp [(H_i - H_L)/RT] \quad (4)$$

is obtained, where subscript L refers to the normal

lattice site and $(H_i - H_L)$ represents the binding energy of hydrogen E_i at trap site i . Equation 4 makes use of the Fermi–Dirac distribution law for both trapped and lattice-dissolved hydrogen [15–18].

Provided rapid hydrogen-assisted cracking occurs in such a manner that the excess hydrogen atoms initially residing at the grain boundaries remain attached to the two newly created free surfaces, with no hydrogen atom exchange with bulk phases, the cohesive energy of the grain boundary γ is given with the help of the Gibbs adsorption theory as follows [19]

$$\begin{aligned} \gamma &= 2\gamma_s - \gamma_b \\ &= 2\gamma_s^0 - \gamma_b^0 - \int_0^{\Gamma_b} \left[\mu_b^{\text{H}}(\Gamma_b) - \mu_s^{\text{H}}(\Gamma_b/2) \right] d\Gamma_b \end{aligned}$$

where the superscript 0 refers to surface energies in the absence of the hydrogen, and Γ_b is the excess number of hydrogen atoms per unit area of grain boundary. This can be written as

$$\gamma = \gamma^0 - n_b^0 N_b \int_0^{\theta_b} \left[\mu_b^{\text{H}}(\theta_b) - \mu_s^{\text{H}}\left(\frac{\theta_b}{2}\right) \right] d\theta_b \quad (5)$$

where γ^0 is equal to $(2\gamma_s^0 - \gamma_b^0)$ and N_b is the number of iron atoms per unit boundary area. From Equations 3a and b,

$$\begin{aligned} \mu_b^{\text{H}}(\theta_b) - \mu_s^{\text{H}}\left(\frac{\theta_b}{2}\right) &= (E_s - E_b) \\ &+ RT \ln \left[\left(\frac{2 - \theta_b}{1 - \theta_b} \right) \right] \end{aligned}$$

is obtained where E_s and E_b are the binding energies of hydrogen to the free surface and grain boundary as trap sites, respectively. Substituting this into Equation 5 and integrating with respect to θ_b , one obtains

$$\begin{aligned} \gamma &= \gamma^0 - n_b^0 N_b \{ (E_s - E_b) \theta_b + RT \\ &\times [\ln 4 + (1 - \theta_b) \ln (1 - \theta_b) - (2 - \theta_b) \\ &\times \ln (2 - \theta_b)] \} \quad (6) \end{aligned}$$

As θ_b approaches zero, γ goes toward γ^0 . When trap sites are completely saturated with hydrogen atoms, that is $\theta_b \simeq 1$, γ has nearly the value of $\gamma^0 - n_b^0 N_b [(E_s - E_b) + RT \ln 4]$.

It is suggested from Equation 6 that the material parameters, such as cohesive energy of hydrogen-free grain boundary γ^0 , planar trap density of grain boundary $n_b^0 N_b$, and binding energies E_s and E_b will considerably influence γ . However, no generally accepted value for the above material parameters at room temperature is available at present. It is therefore reasonable to take γ^0 as values less than 1 J m^{-2} for commercial steels, based on the fact that metalloid impurities such as phosphorus are segregated and reduce the cohesive energy of grain boundaries [20]. If we assume that n_b^0 is unity, $n_b^0 N_b$ is calculated as 1.97×10^{-5} , 2.79×10^{-5} , and $1.14 \times 10^{-5} \text{ mol m}^{-2}$ for $\{100\}$, $\{110\}$ and $\{111\}$ planes, respectively. However, the higher indexed planes have lower values and grain boundaries will have random orientations. Thus the values of γ^0 , $n_b^0 N_b$, and E_s are here taken as

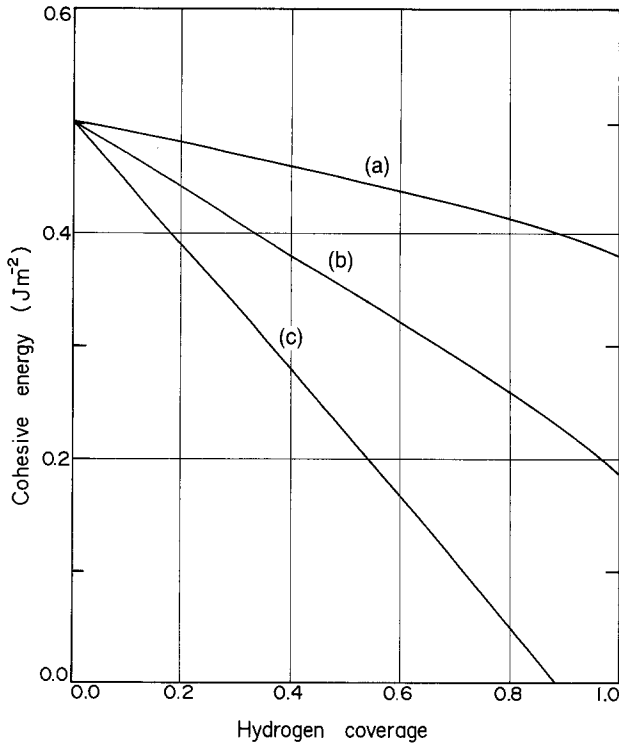


Figure 1 Dependence of cohesive energy of stress-free grain boundary on hydrogen coverage for the cohesive energy of hydrogen-free grain boundary $\gamma^0 = 0.5 \text{ J m}^{-2}$, for several values of trap binding energy of grain boundary E_b : (a) 65, (b) 50, (c) 30 kJ mol^{-1} .

0.5 J m^{-2} , $1.3 \times 10^{-5} \text{ mol m}^{-2}$, and 70.7 kJ mol^{-1} [21], respectively.

The changes of grain boundary cohesive energy γ with varying hydrogen coverage θ_b are plotted in Fig. 1 for several E_b values. If the value of $(E_s - E_b)$ has a value much larger than $RT \ln 4$ (usually this is the case), one obtains a nearly linear relationship between γ and θ_b . This relationship can be expressed as

$$\gamma \simeq \gamma^0 - n_b^0 N_b [(E_s - E_b) + RT \ln 4] \theta_b \quad (7)$$

If the grain boundary is stress-free, or the hydrostatic stress contribution to the chemical potential of the hydrogen atom is negligibly small, the cohesive energy of the grain boundary decreases linearly with the increase of hydrogen coverage. As E_b approaches E_s , however, the γ against θ_b relationship deviates from the straight line, as shown in Fig. 1. This figure also shows that cohesive energy increases with the trap binding energy of the grain boundary. This increase arises from the fact that the difference in the chemical potentials of hydrogen atoms at the grain boundary and the free surface decreases. γ can have a negative value at a certain boundary, when hydrogen coverage and trap-binding energy exceed critical values. The boundaries involving negative γ values become energetically unstable and will decohere even in the absence of externally applied stress. The hydrogen molecules then exert very high internal pressure within the voids due to the high hydrogen fugacity of the environment. The blistering phenomenon, for example, is readily explained using this concept.

In the presence of triaxial stress exerted on the grain boundary, the equilibrium hydrogen concentration

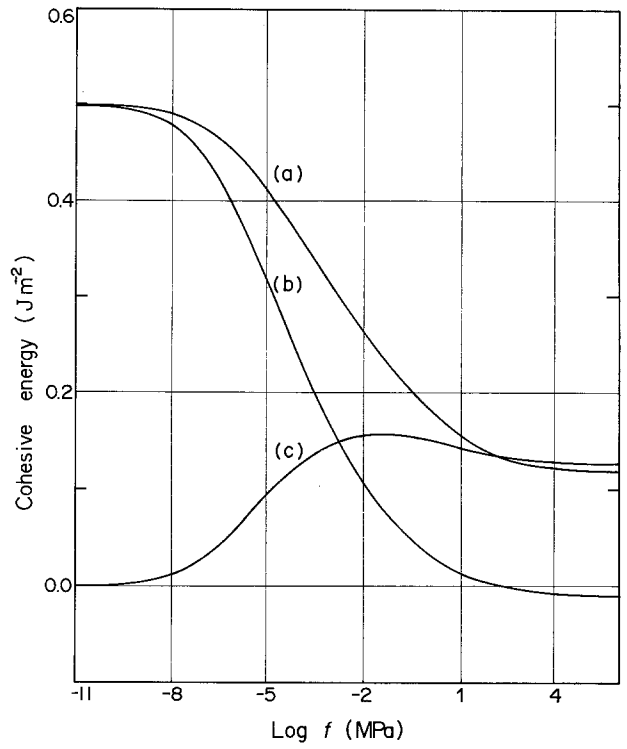


Figure 2 Changes of (a) cohesive energy of grain boundary under a hydrostatic stress field; (b) cohesive energy of stress-free grain boundary; (c) cohesive energy increase due to the hydrostatic stress field, with varying hydrogen fugacity for the trap-binding energy of grain boundary $E_b = 35 \text{ kJ mol}^{-1}$ and yield strength $\sigma_{ys} = 1500 \text{ MPa}$.

increases by the contributions due to the hydrostatic stress field [22–24] as well as due to the trap-binding energy. We designate as E_σ the amount of chemical potential decrease by the hydrostatic stress at the grain boundary. The chemical potential of hydrogen residing at the grain boundary is obtained from Equation 3b as

$$\mu_b^H = (\mu_0^H - H_b - E_\sigma) + RT \ln \left(\frac{\theta_b}{1 - \theta_b} \right) \quad (8)$$

However, since the normal stress component can not be developed on the newly produced free surfaces, μ_s^H is effectively independent of the stress state of grain boundary. In Equation 8, E_σ is given by $\bar{V}_H \sigma_{ii} / 3$, where \bar{V}_H is the partial molar volume of hydrogen in steel. \bar{V}_H is taken as $2 \text{ cm}^3 \text{ mol}^{-1}$ [25, 26]. \bar{V}_H is assumed to be independent of changes in θ_b . Substituting Equation 8 into Equation 5, integration yields

$$\begin{aligned} \gamma = & \gamma^0 - n_b^0 N_b \{ (E_s - E_b - E_\sigma) \theta_b + RT \\ & \times [\ln 4 + (1 - \theta_b) \ln (1 - \theta_b) - (2 - \theta_b) \\ & \times \ln (2 - \theta_b)] \} \end{aligned} \quad (9)$$

The change of fractional coverage of the normal lattice site θ_L with hydrogen fugacity is given by Sievert's law near room temperature [16, 27] as

$$\theta_L = 0.00185 \sqrt{f} \exp \left(- \frac{28600}{RT} \right)$$

Here f is the hydrogen fugacity in MPa. Taking into account the effect of the hydrostatic stress field and noting that θ_L is negligibly small, θ_b is given from

Equation 4 by

$$\frac{\theta_b}{1 - \theta_b} = \frac{\theta_L}{1 - \theta_L} \exp \left[\frac{(E_b + E_\sigma)}{RT} \right] \simeq 0.00185\sqrt{f} \times \exp \left[\frac{(E_b + E_\sigma - 28600)}{RT} \right] \quad (10)$$

The changes of chemical and mechanical contributions of hydrogen to cohesive energy with hydrogen fugacity are presented in Fig. 2. The cohesive energy of the grain boundary under a hydrostatic stress field (curve a) as expressed in Equation 9 is composed of that of the stress-free grain boundary as expressed in Equation 6 (curve b) and the increase due to the hydrostatic stress field (curve c). These calculations were performed for the plane strain condition where σ_{ii} is given by $(1 + \nu)(2\sigma_{yy} - \sigma_{ys})$ [10]. ν and σ_{yy} are Poisson's ratio and the local resolved normal stress, respectively. σ_{ys} , E and a_0 were evaluated as 1500 MPa, 201 GPa, and 0.29 nm respectively.

It is very important to note that the existence of a hydrostatic stress increases the cohesive energy, because the hydrostatic stress field decreases the difference in chemical potential between grain boundary and free surface by the amount E_σ , which causes an increase in cohesive energy by $n_b^0 N_b E_\sigma \theta_b$. The increased amount shows a maximum value at a certain hydrogen fugacity because E_σ decreases and θ_b increases with increasing f . The decrease in chemical potential due to a triaxial stress field is estimated to be at the most about 15 kJ mol^{-1} if \bar{V}_H is taken as $2 \text{ cm}^3 \text{ mol}^{-1}$ for normal lattice sites of high-strength steels. In reality \bar{V}_H at a grain boundary is expected to have a lower value than $2 \text{ cm}^3 \text{ mol}^{-1}$ owing to the open space. Under these circumstances we note that the contribution of the triaxial stress field to the chemical potential of hydrogen at the grain boundary is much smaller, as compared to the effect of trap-binding energy on the chemical potential of hydrogen at the grain boundary.

It is usually understood [6–8, 10, 22] that susceptibility to hydrogen-assisted cracking is determined simply by the decrease of cohesive energy and/or cohesive force of the grain boundary. For example, materials under plane strain conditions show more susceptibility to hydrogen-assisted cracking than those under plane stress conditions. Conventionally, this has been ascribed to the fact that plane strain develops a triaxial stress field, which increases the equilibrium hydrogen concentration in the fracture zone and thus the decrease in cohesive energy of a grain boundary. However, Fig. 2 shows that for the grain boundary under plane strain conditions, the cohesive energy is reduced by hydrogen by a lesser extent than the grain boundary under plane stress conditions. In the case of the plane strain state, the plastic constraint factor shows a much higher value than that for the plane stress state; this causes a higher value of local resolved normal stress ahead of the crack tip at a given stress intensity level. Consequently, the condition of inequality (Equations 1a and b) is so readily met that the material in plane strain is more susceptible to

hydrogen-assisted cracking than that in plane stress, even though the former stress state shows higher cohesive energy than the latter.

3. Dependence of threshold-stress intensity K_{th} on hydrogen fugacity f

In the previous section, the cohesive energy dependence on hydrogen coverage and fugacity has been discussed. To evaluate the K_{th} dependence on hydrogen fugacity, a knowledge of the stress distribution ahead of the crack is required. As an analytic function of stress distribution, the HRR (Hutchinson–Rice–Rosengren) asymptotic stress analysis [28, 29] was employed, despite some errors as compared with the numerical analyses [30–32]. The RKR (Ritchie–Knott–Rice) criterion [33] implies that at $K_I = K_{th}$, σ_{yy} must exceed σ_{th} over a characteristic distance ℓ_0^* directly ahead of the crack tip. The RKR criterion has also been validated for hydrogen-assisted cracking [10, 11]. By applying the RKR criterion, an expression for the threshold stress intensity is obtained [34]:

$$K_{th} = \beta^- [(N + 1)/2] \ell_0^* \frac{1}{2} \left\{ \frac{\sigma_{th}^{[(N+1)/2]}}{\sigma_{ys}^{[(N-1)/2]}} \right\} \quad (11)$$

where

$$\beta = f(N) \left[\frac{(1 - \nu^2)}{\varepsilon_0 I_N} \right]^{1/(N+1)}$$

means the amplitude of the stress singularity, N is the Ramberg–Osgood hardening exponent, I_N and $f(N)$ are numerical constants depending on N , and ε_0 is the yield strain.

ℓ_0^* has not been experimentally determined at present. However, it has been reported that the initiation of hydrogen-assisted cracks occurs within a shorter distance than one grain diameter from the macro-crack tip for sharply precracked specimens [6, 35–37]. Usually the grain size varies widely with the conditions of materials processing and heat treatment. The K_{th} dependence on hydrogen fugacity is relatively insensitive to the choice of ℓ_0^* value in comparison with other parameters, such as cohesive energy, planar trap density and trap-binding energies of grain boundary and free surface. Using Equations 2, 9, 10 and 11 the K_{th} values were calculated as a function of hydrogen fugacity for a ℓ_0^* value of $10 \mu\text{m}$.

The results for the calculated dependence of threshold-stress intensity on hydrogen fugacity for several values of E_b are shown in Fig. 3 at $\sigma_{ys} = 1500 \text{ MPa}$ and $N = 8$. Figure 3 indicates that at relatively low hydrogen fugacity, K_{th} shows a lower value for a larger value of E_b . However, when hydrogen fugacities are sufficiently high for all grain boundaries to be saturated with hydrogen irrespective of E_b values, the opposite applies: K_{th} shows a higher value for a larger value of E_b . This increased K_{th} is due to the reduced difference in chemical potentials of hydrogen between the grain boundary and the free surface. In contrast, Figs 1 and 2 show a clear distinction between the hydrostatic stress contribution and the trap-binding energy contribution to the chemical potential of hydrogen at the grain boundary.

Figure 4 shows the threshold-stress intensity

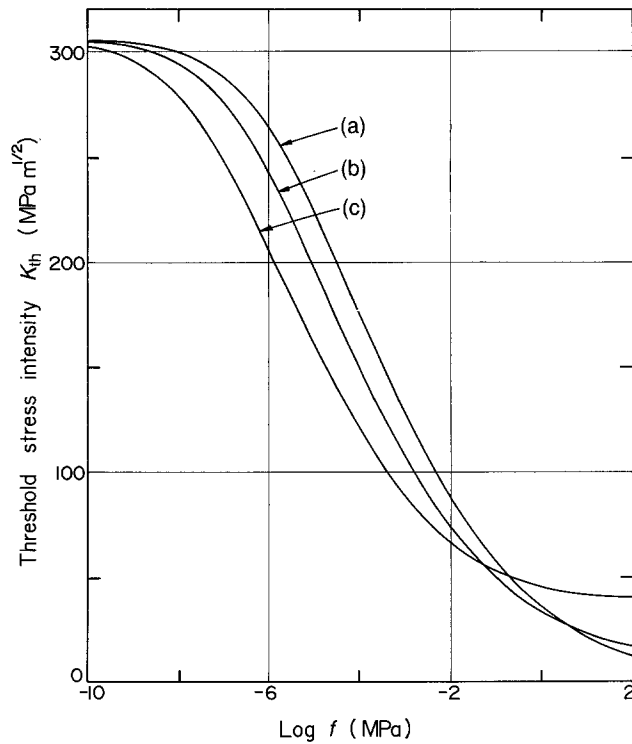


Figure 3 Dependence of threshold-stress intensity K_{th} on hydrogen fugacity f at the yield strength $\sigma_{ys} = 1500$ MPa and work-hardening exponent $N = 8$ for different values of trap-binding energy of grain boundary E_b : (a) 33, (b) 35, (c) 38 kJ mol^{-1} .

dependence on hydrogen fugacity at $N = 8$ and $E_b = 35 \text{ kJ mol}^{-1}$ for different yield strengths. At a constant hydrogen fugacity, the higher yield strength requires the lower K_I level necessary for occurrence of the intergranular hydrogen-assisted cracking. This is based upon the fact that the higher stress intensification ahead of the crack tip is achieved due to the higher yield strength at the same K_I level. This result is consistent with previous experimental observations [3, 38, 39].

Figure 5 presents the effect of the hardening exponent on the K_{th} against $\log f$ at $\sigma_{ys} = 1500$ MPa and $E_b = 35 \text{ kJ mol}^{-1}$. K_{th} decreases with decreasing N . This is explained in a similar way: as N is decreased, the stress elevation is more intensified within the plastically deformed zone.

In this section, we discuss how the material parameters influence the dependence of threshold-stress intensity on hydrogen fugacity derived from a situation where the hydrogen-assisted crack is thermodynamically equilibrated with hydrogen. The results shown in Figs 3 to 5 are consistent with the experimental data of Akhurst & Baker [10], indicating that the threshold-stress intensity dependence on hydrogen fugacity proposed in this work is valid for intergranular hydrogen-assisted cracking. Nonetheless, it is still an open question as to whether this process is crack-initiation controlled or crack-propagation controlled, and as to which microstructural site initiates the hydrogen-assisted crack.

Numerical analyses [30–32] suggest that the maximum stress exists ahead of a sharp crack due to blunting of the crack tip. As the K_I level is raised, the value of the maximum stress is effectively limited and its position moves further away from the crack tip.

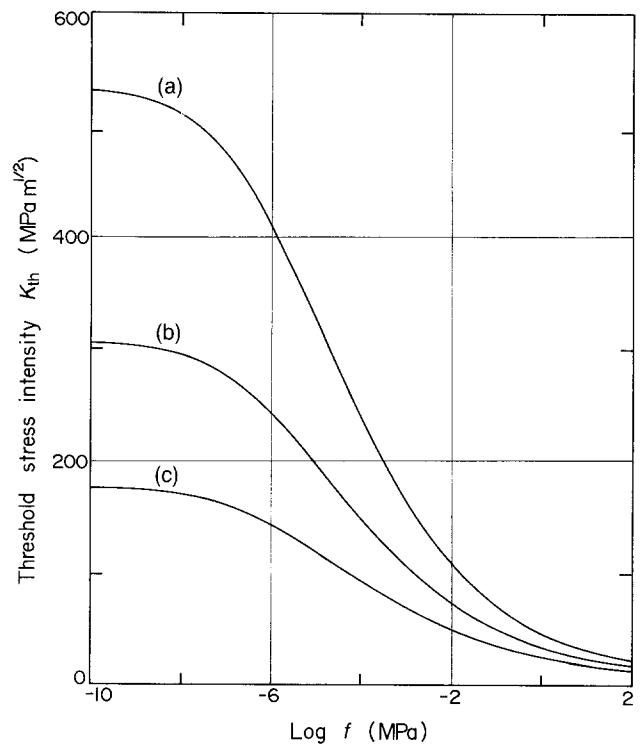


Figure 4 Dependence of threshold-stress intensity K_{th} on hydrogen fugacity f at the work-hardening exponent $N = 8$ and trap-binding energy of grain boundary $E_b = 35 \text{ kJ mol}^{-1}$ for various yield strengths: $\sigma_{ys} =$ (a) 1300, (b) 1500, (c) 1700 MPa.

However, the HRR analysis used in this study does not consider the crack blunting effects. After the position of maximum stress reaches l_0^* , K_{th} derived in this work has no physical significance for intergranular hydrogen-assisted cracking.

4. Fracture mode transition for hydrogen-assisted cracking

Hydrogen-assisted cracking occurs by a delayed failure process which involves hydrogen diffusing into the fracture zone until the hydrogen concentration exceeds a critical value necessary for fracture at a given K_I level. If the K_I level is high, so that micro-voids initiate and grow at interfaces between the matrix and second-phase particles before the hydrogen concentration exceeds the critical value necessary for intergranular fracture, then hydrogen-assisted cracking will occur in the micro-void coalescence mode rather than in the intergranular mode. Hence, the hydrogen-assisted cracking fracture mode requiring the lower hydrogen concentration is operative at a given K_I level.

High-strength steels generally exhibit a fracture mode transition from intergranular at a lower K_I level to micro-void coalescence mode at a higher K_I level [2, 3]. This arises from the higher hydrogen-free threshold-stress intensity K_{th}^0 than the fracture toughness K_{IC} in air. K_{th}^0 is defined as the K_{th} value required for the occurrence of the intergranular fracture mode in the absence of hydrogen. In air, high-strength steels are usually fractured in the micro-void coalescence manner, except for the temper embrittlement process caused by phosphorus, tin, antimony etc. (see below). The fracture mode transition is explained as follows.

The factors affecting the K_{th} necessary for the

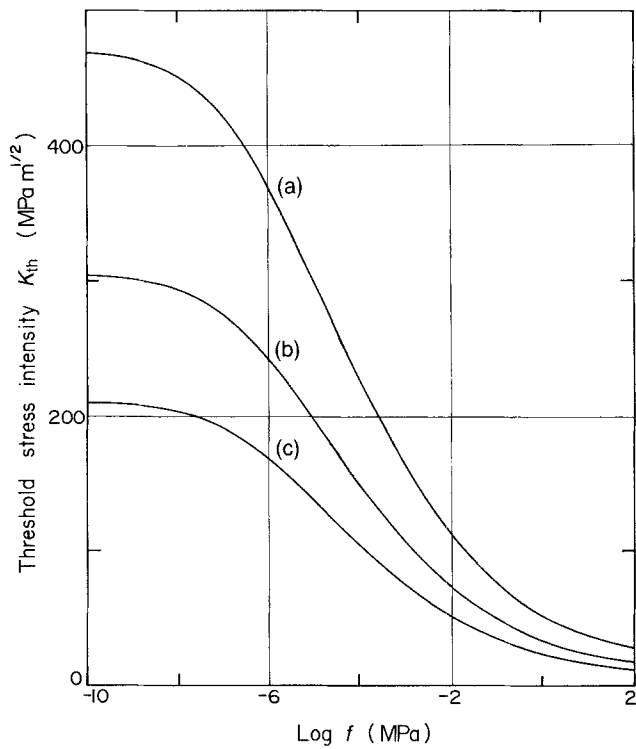


Figure 5 Dependence of threshold-stress intensity K_{th} on hydrogen fugacity f at the yield strength $\sigma_{ys} = 1500$ MPa and trap-binding energy of grain boundary $E_b = 35$ kJ mol⁻¹ for various work-hardening exponents: $N =$ (a) 9, (b) 8, (c) 7.

occurrence of the micro-void coalescence mode include the fracture strain ϵ_f and the yield stress σ_{ys} [34], which are influenced by hydrogen. It is still unknown how the three stages of micro-void coalescence involving initiation, growth and link-up of micro-voids [40] are influenced by hydrogen. Nevertheless, hydrogen can reduce the bond strength of the interfaces between the matrix and second-phase particles, which causes an increase in the number of micro-void initiation sites and thus the decrease in ϵ_f . Presumably the effect of hydrogen on dislocation mobility and thus σ_{ys} is negligibly small.

The condition of inequality Equations 1a and b should be satisfied for the occurrence of intergranular hydrogen-assisted cracking. Because of both the high yield strength and the marked decrease in cohesive energy of a grain boundary caused by the presence of hydrogen, this condition is readily met even at comparatively low K_I levels. Hence the K_{th} necessary for the occurrence of the intergranular mode can have a much lower value than that for the occurrence of the micro-void coalescence mode. Thus the slope of K_{th} -log f curve for the intergranular mode is so steep compared with that for the micro-void coalescence mode that the two curves intersect at K_I^{tr} where a transition of the fracture mode of hydrogen-assisted cracking takes place from the intergranular to the micro-void coalescence manner. This situation is illustrated in Fig. 6.

The cohesive strength of the grain boundary can be reduced to such an extent that the K_{th} necessary for the occurrence of the intergranular mode is always lower than that for the occurrence of the micro-void coalescence mode over all ranges of hydrogen fugacity due to the enrichment of metalloids impurities such as phos-

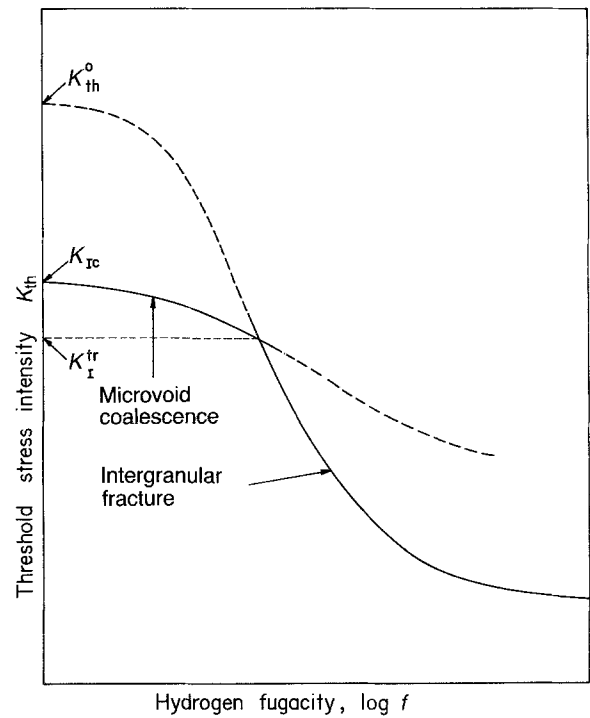


Figure 6 Schematic representation of fracture mode transition for hydrogen-assisted cracking as related to the relationship K_{th} against log f .

phorus, tin, antimony etc. at the grain boundaries during tempering. Then hydrogen-assisted cracking by the intergranular mode is predominant at any test condition of K_I values and hydrogen fugacities. This is experimentally identified [41, 42].

In TEM fractographs of hydrogen-assisted cracking in high-strength steels, the regions for the occurrence of the quasi-cleavage fracture mode have been observed to be located between those representing the intergranular and micro-void coalescence fracture modes [2]. The critical stress concept is valid for describing the quasi-cleavage mode as well as the intergranular mode. However, no data for material parameters such as γ^0 and E_b etc. for the cleavage plane are available at present. Hence a discussion of the fracture mode transition involving the quasi-cleavage mode is beyond the scope of this work.

5. Conclusions

From the above thermodynamic analyses for hydrogen-assisted intergranular cracking, the following conclusions are drawn.

1. Cohesive strength and threshold-stress intensity associated with hydrogen-assisted intergranular fracture are modelled by employing the critical stress and critical hydrogen concentration concepts.

2. A functional relationship between the cohesive energy of decohering grain boundary and the hydrogen concentration was obtained from thermodynamic treatment on the basis of the Gibbs adsorption theorem. In the absence of a hydrostatic stress field, the cohesive energy of a grain boundary decreases linearly with adsorbed hydrogen concentration. However, in the presence of a hydrostatic stress, this linear relationship is not obeyed and the cohesive energy increases by the amount of the hydrostatic stress contribution, contrary to previous suggestions.

3. As trap-binding energy at a grain boundary increases, K_{th} increases in the region where hydrogen coverage approaches unity, whereas K_{th} decreases in the region unsaturated with hydrogen. This is discussed in terms of the difference of the chemical potentials of hydrogen between the grain boundary and the free surface.

4. As the yield strength increases and/or the hardening exponent decreases, the local resolved tensile stress level within the plastic zone is intensified. This gives rise to a decrease in K_{th} at a constant hydrogen fugacity according to the model.

5. The transition of fracture mode with stress intensity is thought to be related to the effects of hydrogen on the K_{th} necessary for the occurrence of the respective fracture modes.

Acknowledgements

The authors are grateful to Professor R. A. Oriani, Corrosion Research Center, University of Minnesota, USA, for useful comments.

References

1. I. M. BERNSTEIN, *Met. Trans.* **1** (1970) 3143.
2. C. D. BEACHEM, *ibid.* **3** (1972) 437.
3. G. SANDOZ, *ibid.* **3** (1972) 1169.
4. M. WATKINS, M. F. BLUEM and J. B. GREER, *Corrosion* **32**(3) (1976) 102.
5. M. GAO and R. P. WEI, *Met. Trans.* **15A** (1984) 735.
6. R. A. ORIANI and P. H. JOSEPHIC, *Acta Met.* **22** (1974) 1065.
7. W. W. GERBERICH, T. LIVNE, X.-F. CHEN and M. KACZOROWSKI, *Met. Trans.* **19A** (1988) 1319.
8. P. DOIG and G. T. JONES, *ibid.* **8A** (1977) 1993.
9. R. THOMPSON, *J. Mater. Sci.* **13** (1978) 128.
10. K. N. AKHURST and T. J. BAKER, *Met. Trans.* **12A** (1981) 1059.
11. S. V. NAIR and J. K. TIEN, *ibid.* **16A** (1985) 2333.
12. J. KAMEDA, *Acta Met.* **34** (1986) 867.
13. H. KITAGAWA and Y. KOJIMA, *Atomistics of Fracture*, Calcatoggio, Corsica, France, 22–31 May 1981, edited by R. M. Latanision and J. R. Pickens (Plenum, New York, 1983) p. 799.
14. A. KELLY, W. TYSON and A. H. COTTRELL, *Phil. Mag.* **15** (1967) 567.
15. R. A. ORIANI, in *Proceedings of a Conference on Fundamental Aspects of Stress Corrosion Cracking*, Ohio State University, 11–15 Sept. 1967, edited by R. W. Staehle, A. J. Forty and D. VanRooyen (NACE, Houston, Texas, 1969) p. 32.
16. N. R. QUICK and H. H. JOHNSON, *Acta Met.* **26** (1978) 903.
17. J. P. HIRTH and B. CARNAHAN, *ibid.* **26** (1978) 1795.
18. R. B. McLELLAN, *ibid.* **27** (1979) 1655.
19. J. P. HIRTH and J. R. RICE, *Met. Trans.* **11A** (1980) 1501.
20. D. F. STEIN, W. C. JOHNSON and C. L. WHITE, in "Grain Boundary Structure and Properties" (Academic, London, 1976) p. 301.
21. E. CHORNET and R. W. COUGHLIN, *J. Catal.* **27** (1972) 246.
22. A. R. TROIANO, *Trans. ASM* **52** (1960) 151.
23. J. C. M. LI, R. A. ORIANI and L. S. DARKEN, *Z. Phys. Chem.* **49** (1966) 271.
24. H. W. LIU, *J. Basic Engng, Trans. ASME* **D92** (1970) 633.
25. R. A. ORIANI, *Trans. AIME* **236** (1966) 1368.
26. H. WAGENBLAST and H. A. WRIEDT, *Met. Trans.* **2** (1971) 1393.
27. J. P. HIRTH, *ibid.* **11A** (1980) 861.
28. J. W. HUTCHINSON, *J. Mech. Phys. Solids* **16** (1968) 13.
29. J. R. RICE and G. R. ROSENGREN, *ibid.* **16** (1968) 1.
30. J. R. RICE and M. A. JOHNSON, in "Inelastic Behavior of Solids" (McGraw Hill, New York, 1970) p. 641.
31. D. M. TRACEY, *J. Engng Mater. Tech., Trans. ASME* **H98** (1976) 146.
32. R. M. McMEEKING, *J. Mech. Phys. Solids* **25** (1977) 357.
33. R. O. RITCHIE, J. F. KNOTT and J. R. RICE, *ibid.* **21** (1973) 395.
34. R. O. RITCHIE, W. L. SERVER and R. A. WULLAERT, *Met. Trans.* **10A** (1979) 1557.
35. M. GAO, M. LU and R. P. WEI, *ibid.* **15A** (1984) 735.
36. J. KAMEDA and C. J. McMAHON Jr, *ibid.* **14A** (1983) 903.
37. J. KAMEDA, *ibid.* **12A** (1981) 2039.
38. H. G. NELSON and D. P. WILLIAMS, in *Proceedings of a Conference on Stress Corrosion Cracking and Hydrogen Embrittlement of Iron Base Alloys*, Unieux-Firminy, France, 12–16 June 1973, edited by R. W. Staehle, J. Hochmann, R. D. McCright and J. E. Slater (NACE, Houston, Texas, 1977) p. 390.
39. R. VISWANATHAN and S. J. HUDAK, *Met. Trans.* **8A** (1977) 1633.
40. R. GARBER, I. M. BERNSTEIN and A. W. THOMPSON, *ibid.* **12A** (1981) 225.
41. K. YOSHINO and C. J. McMAHON Jr, *ibid.* **5** (1974) 363.
42. C. L. BRIANT, H. C. FENG and C. J. McMAHON Jr, *ibid.* **9A** (1978) 625.

Received 15 May 1988
and accepted 17 January 1989